Specific heat in magnetic field and magnetocaloric effects of α-R2S3 (R = Tb, Dy) single crystals

Specific Heat in Magnetic Field and Magnetocaloric Effects of α-R_2S_3 (R = Tb, Dy) Single crystals

Q. Guo[1], O. Tegus[2] and S. Ebisu[1]*

[1]Division of Applied Sciences, Muroran Institute of Technology, 27-1, Mizumoto-cho, Muroran, Hokkaido 050-8585, Japan

[2]Inner Mongolia Key Laboratory for Physics and Chemistry of Functional Materials, Inner Mongolia Normal University, Hohhot 010022, China

*Corresponding author. Tel.: +81-143-46-5620;
E-mail address: ebisu@mmm.muroran-it.ac.jp (S. Ebisu).

Abstract: The magnetocaloric effects (MCE) of α-Tb_2S_3 and α-Dy_2S_3 single crystals exhibiting successive antiferromagnetic (AFM) transitions have been investigated by analyzing specific heat measured in magnetic field. The temperature dependence of specific heat in the vicinity of the successive transitions shows obvious distinction depending on the orientations of the applied magnetic field for both α-Tb_2S_3 and α-Dy_2S_3 that having orthorhombic crystal structures. When the magnetic field is increased, the specific heat is as follows: For α-Tb_2S_3 in $\boldsymbol{H}//\boldsymbol{b}$, the peak around T_{N2} shifts to lower temperature but the other one peak around T_{N1} barely moves; In $\boldsymbol{H}\perp\boldsymbol{b}$, the peak around T_{N2} has no shift almost within 3 T but suddenly moves to lower temperature in 4 T and the other one peak around T_{N1} shifts to lower temperature in specific heat versus temperature. In the case of α-Dy_2S_3, the two peaks around T_{N2} and T_{N1} shift to lower temperatures in $\boldsymbol{H}//\boldsymbol{b}$ but move to higher temperatures when the magnetic field is increased up to 5 T by $\boldsymbol{H}\perp\boldsymbol{b}$ in spite of antiferromagnetic transitions. Therefore, the maximum value and corresponding temperature of both isothermal magnetic entropy change (ΔS_m) and adiabatic temperature change (ΔT_{ad}) in the magnetic field $\boldsymbol{H}\perp\boldsymbol{b}$ are extremely different in low temperature range from that in the field of $\boldsymbol{H}//\boldsymbol{b}$. The results propone that the MCE of α-Tb_2S_3 and α-Dy_2S_3 could be controlled at low temperature by the magnitude and orientation of magnetic field. It also indicates that the refrigerating capacity and thermal absorption capacity will be controlled by changing magnitude and orientation of magnetic field on the α-Tb_2S_3 and α-Dy_2S_3 single crystals.

Keywords: Rare earth sulfides, Specific heat, Magnetocaloric effect, Successive magnetic phase transition

1 Introduction

Since the magnetic refrigeration technology based on the magnetocaloric effects (MCE) have thrived in the last decade and many magnetic materials with the giant MCE have been investigated for better cooling efficiency and environmental friendliness. For example, $Gd_5(Ge_{1-x}Si_x)_4$ with $0.3 \leq x \leq 0.5$ compounds display giant MCE due to its first-order structural and magnetic phase transition [1]. The $MnFeP_{0.45}As_{0.55}$ compound with Fe_2P-type structure also shows the giant MCE due to a first-order magnetic phase transition and the maximal magnetic entropy change is 14.5 $JK^{-1}kg^{-1}$ and 18 $JK^{-1}kg$ for magnetic field change of 2 T and 5 T at 300 K [2]. The $LaFe_{13-x}Si_x$ compounds ($1.2 \leq x \leq 1.6$) undergo a first-order field induced itinerant-electron metamagnetic transition, so the compounds possess large MCE [3]. The RCo_2 (R = Er, Ho, Dy) alloys exhibit first-order magnetic transition and large MCE. The effects of element substitutions and pressure on RCo_2-based compounds for MCE are also reported [4]. The MCE of RAl_2 (R = Nd and Tm) single crystals with PM-FM transition are reported and the maximal magnetic entropy change in field change of 0-7 T is 35.9 and 8.9 $JK^{-1}kg^{-1}$ at its Curie temperature 6.0 and 76.5 K for $TmAl_2$ and $NdAl_2$, respectively [5].

Recently, the series compounds of α-R_2S_3 (R = rare earth elements) become attractive for their novel physical properties related to magnetic transitions [6-17]. The α-R_2S_3 (R = La-Dy, except Pm and Eu) have an orthorhombic crystal structure (space group *Pnma*), as shown in Fig. 1: there are two crystallographically inequivalent R sites labeled $R1$ and $R2$ in this structure; Atoms on $R1$ with buckling in *ab* plane, where $R2$ atoms are connected to this plane [6, 7, 12 and 15]. Ebisu *et al*., discovered that α-R_2S_3 single crystal showed a novel antiferromagnetic transition at 10 K with anisotropic behavior in the temperature dependence of magnetic susceptibility [6]. Neutron Diffraction data [18] of α-Gd_2S_3 demonstrated that the magnetic unit cell was the same as the chemical unit cell. The heat capacity versus temperature of α-Gd_2S_3 single crystal shows a sharp anomaly at about 10 K, which also means magnetic moments of both Gd1 and Gd2 site order the same temperature [7]. The specific heat of α-Gd_2S_3 is high and likely to be used as regenerator material [16]. Then, the magnetic entropy change is also large and the α-Gd_2S_3 can be a candidate of refrigerant materials. In contrast with α-Gd_2S_3, the α-Tb_2S_3 single crystal exhibits successive antiferromagnetic (AFM) transitions at T_{N1} = 12.5 K and T_{N2} = 3.5 K [14]. The two transitions occur in Tb1 and Tb2 sites, respectively [19]. For α-Dy_2S_3 single crystal, the successive AFM transitions occur at their Neèl temperatures 11.4 and 6.4 K and that the two peaks shifted to different directions depending on the applied magnetic field [14]. When the magnetic

field (up to 2 T) was applied parallel with the *b*-axis those shifted toward lower temperature side, while those shifted to higher temperature side in the magnetic field perpendicular to the *b*-axis.

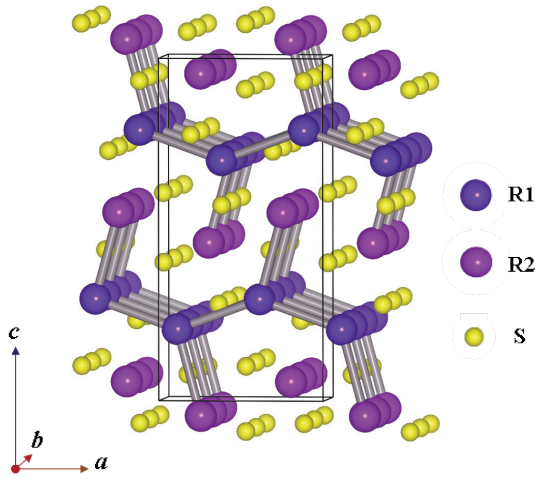

Fig. 1 The crystal structure of α-R_2S_3 compound: rare earth atoms are connected by banding and sulfurs atoms are free.

In the present study, we have investigated magnetic field effects on the specific heat of α-Tb_2S_3 and α-Dy_2S_3 single crystals in the vicinity of the successive magnetic transitions. Although the effect for α-Dy_2S_3 was reported previously [14], the range of applied magnetic field has been extended up to 5 T and the lowest temperature has been extended down to 0.4 K. The magnetocaloric effects (MCE) of α-Tb_2S_3 and α-Dy_2S_3 compounds were estimated from specific heat in magnetic field applied along the *b*-axis and perpendicular to the *b*-axis. The MCE, which expressed by magnetic entropy change and adiabatic temperature change, and the possibility of controlling the MCE in α-Tb_2S_3 and α-Dy_2S_3 single crystals in low temperature by the magnitude and orientation of magnetic field were discussed in this paper.

2 Experimental

Polycrystalline powder samples of α-Tb_2S_3 and α-Dy_2S_3 were synthesized by sulfurizing the powder materials of Tb_4O_7 and Dy_2O_3 (both 99.9 %) on an alumina boat at a temperature in 1223-1273 K under the flow of the argon gas containing CS_2 [6]. The single crystals were grown from the powder sample by a chemical transport reaction method using iodine as a carrier [6]. The crystal structure and single crystal orientation were confirmed by X-ray diffraction measurements using Cu K_α-radiation. The specific heat was measured by using Physical Property Measurement System (PPMS, Quantum Design). The magnetic field in the specific heat measurements was applied to two directions of parallel and perpendicular to the *b*-axis ($\boldsymbol{H} \perp \boldsymbol{b}$ and $\boldsymbol{H} // \boldsymbol{b}$).

The specific heat of α-Tb_2S_3 was measured in the temperature range of 2.0-300 K in no magnetic field and in the temperature range of 2.0-20 K in the magnetic fields within 4 T. The specific heats of α-Dy_2S_3 were measured in the temperature range of 0.7-300 K in no magnetic field and in range of 0.4-20 K in the magnetic fields within 5 T. The isothermal magnetic entropy change and adiabatic temperature change were evaluated from the specific heat data in the magnetic field. Stick-shaped single crystals with hexangular cross sections were used for the specific heat measurements. The α-Tb_2S_3 sample had the mass of 2.2 mg and the length of 2.0-mm along the *b*-axis and the maximum length 0.8-mm in the cross section of the *ac*-plane. While the α-Dy_2S_3 sample had a weight of 2.5 mg, a 1.5-mm length along the *b*-axis and a 0.7-mm maximum-length in *ac*-plane.

3 Results and Discussion

3.1 Confirmation of crystal structure and crystal plane

The X-ray diffraction patterns for powder samples of α-Tb_2S_3 and α-Dy_2S_3 were analyzed at the room temperature and the refinement showed that both of them were single phase having orthorhombic structure with the space group *Pnma*. The lattice parameters were a = 0.7303 nm, b = 0.3900 nm and c = 1.5202 nm for α-Tb_2S_3 and a = 0.7282 nm, b = 0.3878 nm and c = 1.5140 nm for α-Dy_2S_3. The crystal faces of six-side planes of the hexangular stick-shaped single crystals were determined by the X-ray diffraction method. Whenever of these experiments, one set of opposed planes is certainly (001) plane for both α-Tb_2S_3 and α-Dy_2S_3.

3.2 Specific heat

Fig. 2 shows temperature dependence of the molar specific heat for α-Tb_2S_3 under no magnetic field in the temperature range from 2 to 300 K. The solid curve represents the experimental specific heat C_p. It demonstrates two sharp peaks at the successive AFM transitions temperatures T_{N1} = 12.5 K and T_{N2} = 3.5 K [9] as clearly seen in the inset. The dashed straight line shows the Dulong-Petit law, thus it has a value of $C = 3R \times 5$ = 125 $JK^{-1}mol^{-1}$, which R is the gas constant and five is number of atoms in the chemical formula unit of α-Tb_2S_3. The lattice specific heat C_{lat} was estimated by fitting data to the Debye model with the Debye temperature Θ_D = 270 K and shown by dashed curve in Fig. 2. Then, the C_{lat} can be expressed by the following equation:

$$C_{\mathrm{lat}} = 9rN_{\mathrm{A}}k_{\mathrm{B}}\left(\frac{T}{\Theta_{\mathrm{D}}}\right)^3 \int_0^{\frac{\Theta_{\mathrm{D}}}{T}} \frac{x^4 e^x}{(e^x-1)^2} dx, \quad (1)$$

which r is 5, the number of atoms in the chemical formula unit. N_A and k_B are the Avogadro constant and the Boltzmann constant. The Debye temperature Θ_D = 270 K is closer to the value 317 K for α-La_2S_3 as reported by Gschneidner. Jr, et al. [20] rather

than the value 370 K estimated for α-Dy_2S_3 [14]. Although the calculated curve does not fit well

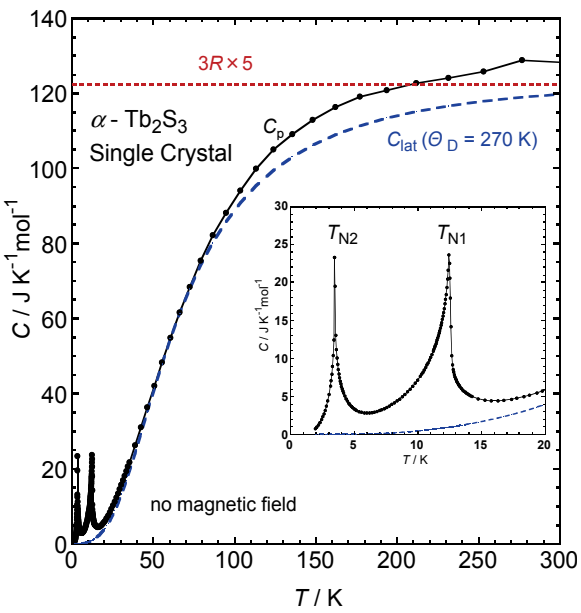

Fig. 2 Temperature dependence of the molar specific heat of α-Tb_2S_3.

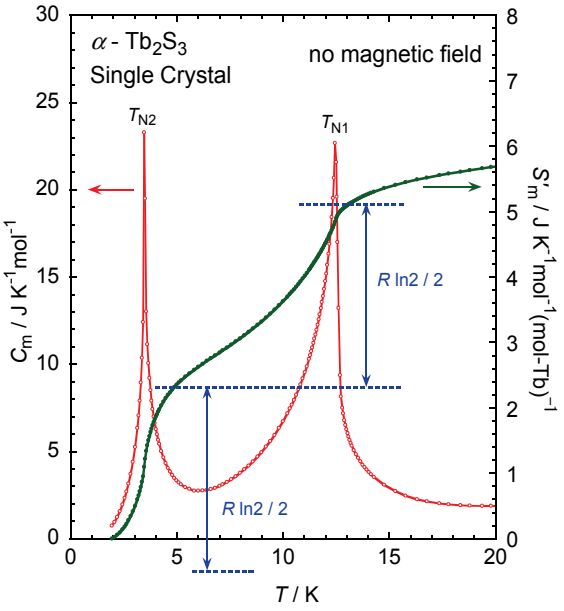

Fig. 3 Temperature dependences of the magnetic specific heat C_m and the magnetic entropy S'_m per mol-Tb.

the C_p curve in the higher temperature range than 90 K, it acceptable well in the lower temperature range. The value of C_{lat} is sufficiently smaller than the C_p in low temperature range. For example, when the value of C_{lat} at the temperature below T_{N1} is less than 5% of C_p for α-Tb_2S_3 and 0.9% for α-Dy_2S_3. It is assumed that the specific heat C_p consists of the lattice contribution C_{lat} and a magnetic one C_m,

$$C_p = C_{lat} + C_m, \qquad (2)$$

because the electrical properties are not metallic in the lower temperature range [9]. The molar magnetic specific heat C_m was obtained by subtracting C_{lat} from C_p is shown in Fig. 3. The magnetic entropy $S'_m(T)$ per mol-Tb is also shown in Fig. 3. It should be noted that the $S'_m(T)$ actually the change from T_0 = 2 K, which is the lowest temperature in the measurement. Therefore, it is evaluated from the following equation:

$$S'_m(T) = \int_{T_0}^{T} \frac{C_m}{2T} dT \ , \qquad (3)$$

Here, the C_m is divided by 2 because α-Tb_2S_3 has two Tb-atoms in a unit formula. The $S'_m(T)$ curve demonstrates large increases around two transitions. Two horizontal dashed lines are drawn across the "shoulders" of the $S'_m(T)$ curve. The temperatures

of intersections are 5.0 and 13.0 K. The magnetic entropy increased by the value of Rln2/2 between these temperatures. It proposes that the Tb^{3+} on Tb1 sites of which magnetic moments order at T_{N1} [19] have pseudo-doublet as a ground state. As for the T_{N2} transition, the value of $S'_m(T)$ at 5.0 K is less than Rln2/2. However, the C_m has a finite value about 0.5 $JK^{-1}mol^{-1}$ at T_0. Therefore, the entropy change below T_0 should be taken into account. If it is estimated that the entropy change across the T_{N2} transition from the horizontal dashed line under the T-axis, the value corresponding to Rln2/2 is obtained. The ground term of a Tb^{3+} on Tb2 site is also considered as a pseudo-doublet. In the crystal structure of this series of α-R_2S_3 compounds, both $R1$ and $R2$ sites have only the mirror symmetry of C_{1h}. Thus, the ground term of the Tb^{3+} having the electron configuration of $4f^8$ separates into 13 singlets. However, there are close two singlets from pseudo-doublet for Tb^{3+} on both the sites of α-R_2S_3. While, Dy^{3+} having the $4f^9$ configuration on have Kramers doublets, which is deduced from the analysis of the specific heat for α-Dy_2S_3 [14].

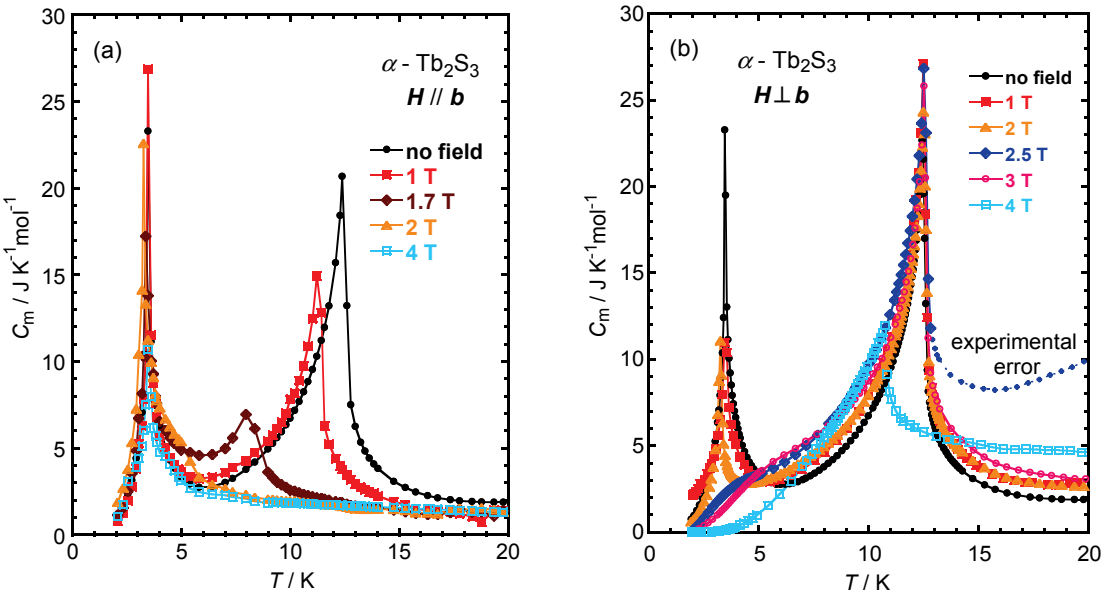

Fig. 4 Temperature dependence of the magnetic specific heat for α-Tb_2S_3 single crystal in various magnetic fields within 4 T ***H*//*b*** (a) and ***H*⊥*b*** (b).

The effect of magnetic field on the specific heat will be discuss. Fig. 4 shows the temperature dependence of the magnetic molar specific heat of α-Tb_2S_3 single crystal in various magnetic fields within 4 T: ***H*//*b*** (Fig. 4a); ***H*⊥*b*** (Fig. 4b). In Fig. 4(a), it can be clearly seen that the T_{N1} peak shifts to lower temperature with increasing the magnetic field up to 1.7 T and then the T_{N1} peak disappears for the magnetic field higher than 2 T. The height of the T_{N1} peak also reduces with the magnetic field increasing up to 1.7 T.

While, the T_{N2} peak does not seriously shift and the maximal value of T_{N2} peak diminishes when the magnetic field is increased. The data for 2.5 and 3 T are not shown in here. In Fig. 4(b), it should be noted that the data of 2.5 T in temperature range above 13 K indicates by the dotted curve and includes large experimental error. In the case of $\boldsymbol{H} \perp \boldsymbol{b}$, the T_{N1} peak is constant about the appearing temperature and the height when the magnetic field is increased up to 3 T. However, it suddenly shifts to lower temperature and decreases by about half in the height when the magnetic field is 4 T. The stability of the T_{N1} peak within the magnetic field of 3T perpendicular to the *b*-axis is consistent with orientation of the ordered Tb1 moments parallel to the *b*-axis [19]. The T_{N2} peak for 2 T appears actually at slightly lower temperature than one for no magnetic field. However, the peak disappears when the magnetic field gets to be higher than 2.5 T. It should be noted that the C_m value at $T = 2$ K, $\mu_0 \boldsymbol{H} = 1$ T ($\boldsymbol{H} \perp \boldsymbol{b}$) is rather large than the values of the other curves in Fig. 4(a) and 4(b). It suggests that the magnetic system under the magnetic field of 1 T in the direction of $\boldsymbol{H} \perp \boldsymbol{b}$ keeps a certain of freedom-degree.

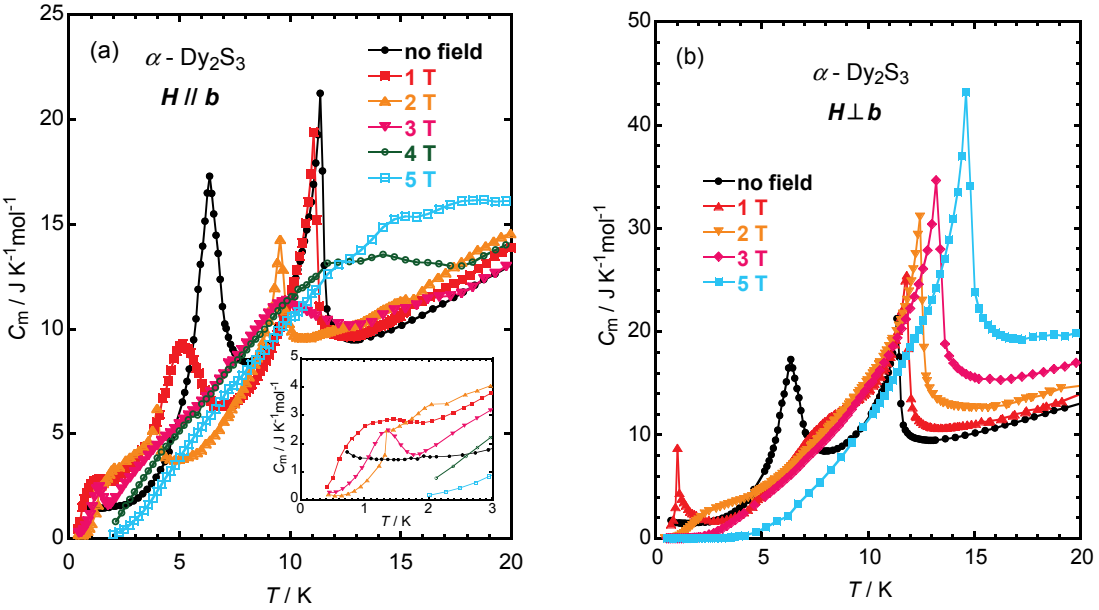

Fig. 5 Temperature dependence of the magnetic specific heat for α-Dy_2S_3 single crystal in various magnetic fields within 5 T $\boldsymbol{H}//\boldsymbol{b}$ (a) and $\boldsymbol{H} \perp \boldsymbol{b}$ (b).

As for α-Dy_2S_3, Ebisu *et al*., have already reported the specific heat under the magnetic field within 2 T and in the temperature range higher than 2 K [14]. However, it will be shown the specific heat measured in the extended range; the magnetic field within 5 T and the temperature down to 0.7 K, in order to investigate MCE. Fig. 5 shows temperatures dependence of the magnetic molar specific heat of α-Dy_2S_3 in the

temperature range below 20 K down to 0.7 or 2.0 K and in the magnetic field up to 5 T; $\boldsymbol{H}//\boldsymbol{b}$ (Fig. 5(a)) and $\boldsymbol{H}\perp\boldsymbol{b}$ (Fig. 5(b)). According to our recent study, the specific heat of α-Dy_2S_3 shows large anisotropy also in the *ac*-plane. It should be pointed out that the specific heat data in Fig. 5(b) are the well resemble data for $\boldsymbol{H}//\boldsymbol{a}$ taken in the recent study. From Fig. 5(a), it can be seen that both T_{N1} and T_{N2} peaks shift to lower temperature and the heights of both peaks reduce by increasing the applied field up to 3 T in $\boldsymbol{H}//\boldsymbol{b}$. But, the both peaks disappear in the field equal and larger than 4 T. However, in Fig. 5(b), T_{N1} peak shifts to higher temperature and its height increases with increasing the magnetic field up to 5 T in $\boldsymbol{H}\perp\boldsymbol{b}$ despite that an AFM transition occurs. It is likely that the gain of the Zeeman term brought about by aligning of the magnetic moments on Dy2 site below T_{N1} assists the shift of T_{N1} peak toward higher temperature. On the other hand, the T_{N2} peak disappears in magnetic field equal and higher than 1 T. Here, it should be pointed out that the C_m under no magnetic field, which is shown in both figures, has finite value at 0.7 K and does not seem to go to zero below 0.7 K. It suggests that a certain of freedom-degree remains below 1 K in no magnetic field, however it seems to disappear in the magnetic field as shown in both figures. This freedom-degree seems to disappears with some magnetic ordering demonstrated as broad peaks around 1-2 K in the curves of 1, 2, 3 T in Fig. 5 (a) and sharp / broad peaks in the curves of 1 / 2 T in Fig. 5(b). It has been reported that Dy^{3+} on one Dy site in which Dy^{3+} moments order at T_{N2} has a doublet ground state because the entropy change across T_{N2} deduced from specific heat data taken in the temperature range higher than 2 K is nearly equal to Rln2. However, it has been clear that the magnetic entropy remains also below 2 K in the present study. Therefore, the ground state of this Dy site might have quasi-quartet ground state.

3.3 Magnetic entropy change and adiabatic temperature change

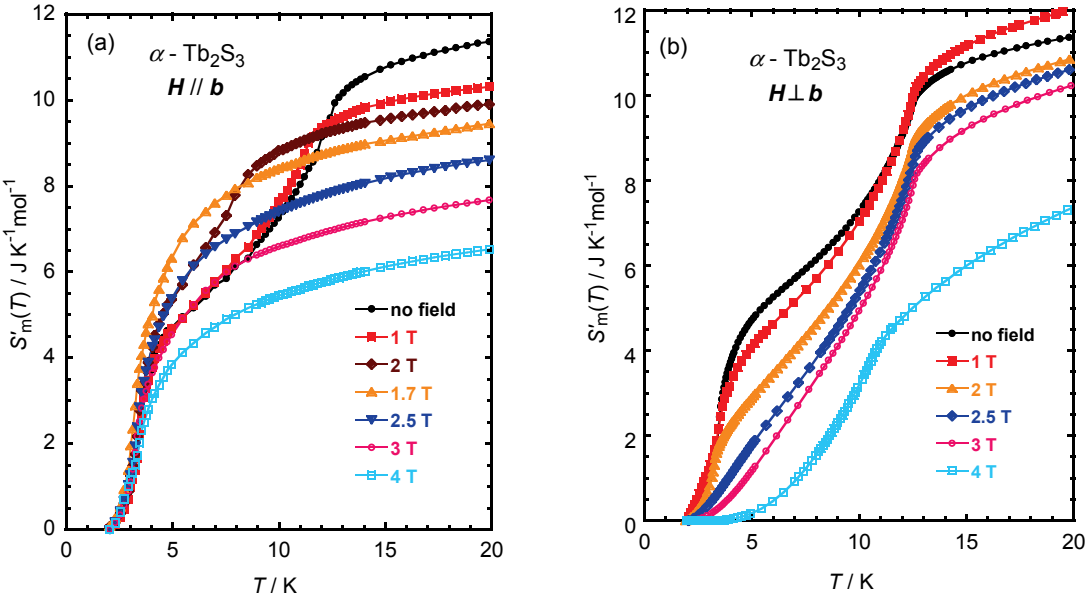

Fig. 6 Temperature dependence of the magnetic entropy for α-Tb_2S_3 single crystal in various magnetic fields within 4 T $\boldsymbol{H}//\boldsymbol{b}$ (a) and $\boldsymbol{H}\perp\boldsymbol{b}$ (b).

Fig. 6 shows the temperature and magnetic field dependence of magnetic entropy, $S'_m(T)$, of α-Tb_2S_3 in magnetic field within 4 T ($\boldsymbol{H}//\boldsymbol{b}$ and $\boldsymbol{H}\perp\boldsymbol{b}$), which was calculated by Eq. (3) substituting 2 K for T_0. The characteristic change of $S'_m(T)$ by increasing magnetic field is shown for the case of $\boldsymbol{H}//\boldsymbol{b}$ in Fig. 6 (a). While the $S'_m(T)$ decreases with increasing field is complicated below 12.2 K. In Fig. 6(b), the data for $\mu_0\boldsymbol{H}$ = 1 T has been excluded. Because the C_m has rather large value at 2 K only in the case for $\mu_0\boldsymbol{H}$ = 1 T as mentioned above, a simple comparison of $S'_m(T)$ evaluated from the C_m data above 2 K between the case for 1 T and the other cases is not adequate. As a consideration, the $S'_m(T)$ was evaluated for $\mu_0\boldsymbol{H}$ = 2.5 T assuming that the C_m for 2.5 T above 13 K, including experimental errors, was as same as the C_m for $\mu_0\boldsymbol{H}$ = 3 T in Fig. 4(b).

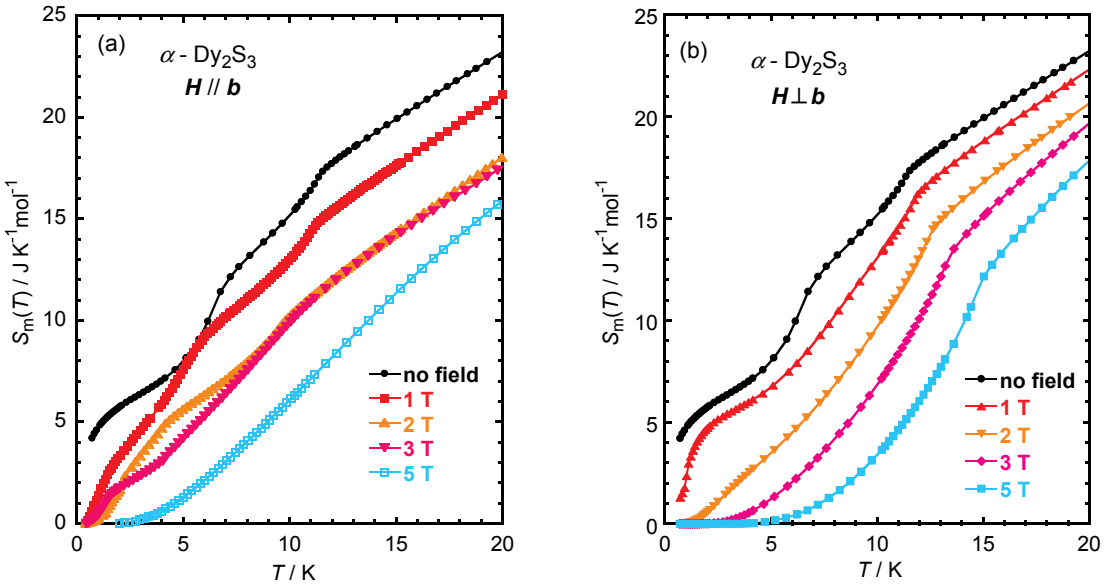

Fig. 7 Temperature dependence of the magnetic entropy for α-Dy_2S_3 single crystal in various magnetic fields within 5 T $\boldsymbol{H}//\boldsymbol{b}$ (a) and $\boldsymbol{H}\perp\boldsymbol{b}$ (b).

Fig. 7 shows the temperature and magnetic field dependence of $S_m(T)$ of α-Dy_2S_3 in magnetic field $\boldsymbol{H}//\boldsymbol{b}$ (Fig. 7(a)) and $\boldsymbol{H}\perp\boldsymbol{b}$ (Fig. 7(b)) from 0 to 5 T. The $S_m(T)$ is defined as

$$S_m(T) = S'_m(T) + S_0 \quad , \tag{4}$$

where the S_0 is the magnetic entropy below T_0 and evaluated by

$$S_0 = \int_0^{T_0} \frac{C_m}{2T} dT \quad . \tag{5}$$

The S_0 should be considered in the case of α-Dy_2S_3. The C_m values at T_0 for $\mu_0\boldsymbol{H}$ = 1, 2, 3, 4 and 5 T in Fig. 5(a) are sufficiently small and tend to go to zero with decreasing temperature; hence, it is assumed that the S_0 values for these cases are zero. Similarly, judging from the C_m values at T_0 in Fig. 5(b), it can be assumed that the S_0 values for $\mu_0\boldsymbol{H}$ = 2, 3, 5 T are zero. However, the S_0 cannot be neglected for $\mu_0\boldsymbol{H}$ = 0 and 1 T ($\boldsymbol{H}\perp\boldsymbol{b}$). In order to evaluate S_0 for these cases, the C_m model is shown in Fig. 8. In the case of $\mu_0\boldsymbol{H}$ = 1 T, the C_m tends to go to zero with decreasing temperature to zero; therefore, we assume the straight broken line C_{mB} for the magnetic specific heat below T_0. From this assumption S_{0B} is evaluated as 2.1 $JK^{-1}mol^{-1}$. While T goes to zero, the C_m in no magnetic field does not seem to get to zero. Hence, we assume the C_{mA} consisting of two connected broken lines for upper limit of magnetic specific heat. The temperature of the connecting point T_1 is taken as $T_0/2$. The S_0 calculated from C_{mA}, S_{0A}, is 6.1 $JK^{-1}mol^{-1}$. It is assumed that the S_0 for the case of no field is smaller than S_{0A} and larger

than S_{0B}. We calculated the S_0 by the equation; $S_0 = (S_{0A}+S_{0B})/2$, as 4.1 $JK^{-1}mol^{-1}$. The $S_m(T)$ for no magnetic field and 1 T ($\boldsymbol{H}\perp\boldsymbol{b}$) are taken S_0 into consideration in Fig. 7. Consequently, the $S_m(T)$ for no field at 6.4 K is nearly equal to Rln4. The quasi-quartet ground state model for one Dy site that mentioned above seems to be adequate. In both Fig. 7(a) and Fig. 7(b), it can be seen that the magnetic entropy decreases with increasing the magnetic field.

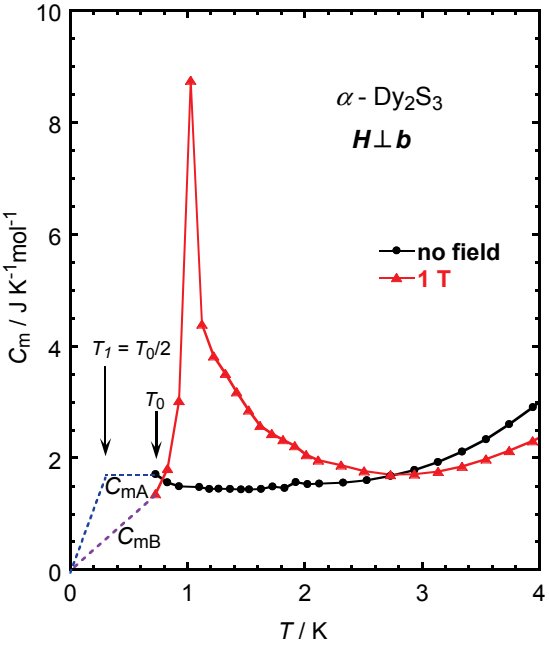

Fig. 8 The C_m model for evaluating magnetic entropy of α-Dy_2S_3 below T_0.

The magnetic entropy change will be discussed under the magnetic field. Fig. 9 shows the temperature and magnetic field dependence of magnetic entropy change, $-\Delta S_m(T, H)$, of α-Tb_2S_3; $\boldsymbol{H}//\boldsymbol{b}$ (Fig. 9(a)), $\boldsymbol{H}\perp\boldsymbol{b}$ (Fig. 9(b)). It was calculated by following equation,

$$-\Delta S_m(T,H) = -[S'_m(T)_H - S'_m(T)_{H=0}]. \quad (6)$$

In the case of $\boldsymbol{H}//\boldsymbol{b}$, it can be seen in Fig. 9(a) that the valley of magnetic entropy change having negative values is formed below 12 K when the magnetic field change is equal to or smaller than 2 T. It is due to existing the complicated phases of $S'_m(T)$ in Fig. 6(a). It is largely different from the positive values in the case of $\boldsymbol{H}\perp\boldsymbol{b}$. This inverse MCE was also reported in RCu_2 (R = Tb, Dy, Ho, Er) compounds which has also successive transitions [20]. The $-\Delta S_m(T, H)$ in the range of 12-20 K increases with increasing magnetic field change up to 4 T. The maximal $-\Delta S_m(T, H)$ of α-Tb_2S_3 is 12.0 $Jkg^{-1}K^{-1}$at 20 K in magnetic field change of 4 T. On the other hand, the $-\Delta S_m(T, H)$ for $\boldsymbol{H}\perp\boldsymbol{b}$ increases with increasing magnetic field change up to 4 T in the wide temperature range

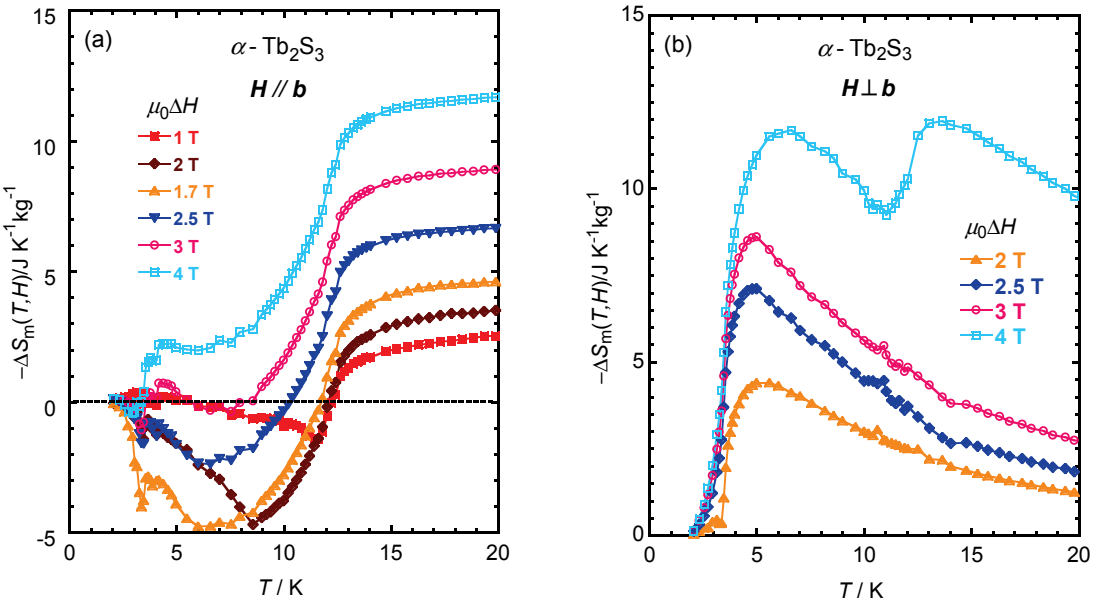

Fig. 9 Temperature dependence of the magnetic entropy change for α-Tb_2S_3 single crystals in magnetic field change within 4 T ***H*//*b*** (a) and ***H*⊥*b*** (b).

above 4 K, as shown in Fig. 9(b). It can be seen obviously that two peaks of $-\Delta S_m(T, H)$ emerges under the magnetic field change of 4 T, compared with one peak in ΔH of 2, 2.5 and 3 T. Consequently, the $-\Delta S_m(T, H)$ in $\mu_0\Delta H$ of 4 T keeps large value in a broad temperature range, which gets more than twice as large as that in $\mu_0\Delta H$ of 2, 2.5 and 3 T in the temperature range above 12 K. The maximal value of magnetic entropy change for α-Tb_2S_3 is $-\Delta S_m(T, H) = -\Delta S_m(13\ K, 4\ T) = 12.0\ Jkg^{-1}K^{-1}$ in the measurement range. Comparing the cases of ***H*//*b***; Fig. 9(a) and ***H*⊥*b***; Fig. 9(b), the $-\Delta S_m(T, H)$ of α-Tb_2S_3 single crystal shows fairly large differences in shape and feature. Therefore, the α-Tb_2S_3 single crystal has potential to control the large MCE by rotating the single crystal in a magnetic field.

For the α-Dy_2S_3, the temperature dependence of $-\Delta S_m(T, H)$ in $\mu_0\Delta H$ from 1 to 5 T in ***H*⊥*b*** and ***H*//*b*** is shown in Fig. 10(a) and (b). The magnetic entropy change of α-Dy_2S_3 increases in both cases ***H*⊥*b*** and ***H*//*b*** with increasing magnetic field change. There are almost flat peak in both conditions ***H*⊥*b*** and ***H*//*b*** in the temperature range from 7 to 12 K in the case of $\mu_0\Delta H$ = 5 T. The half-peak temperature width of α-Dy_2S_3 also makes larger in ***H*⊥*b*** and ***H*//*b*** with increasing magnetic field change. The maximal $-\Delta S_m(T, H)$ of α-Dy_2S_3 is 22.8 $Jkg^{-1}K^{-1}$at 11.7 K in magnetic field of 5 T (***H*//*b***) and 28.3 $Jkg^{-1}K^{-1}$ at 11.4 K in magnetic field of 5 T (***H*⊥*b***). Comparing Fig. 10(a) and (b), the $-\Delta S_m(T, H)$ of α-Dy_2S_3 single crystal shows large difference in value depending on the magnetic field direction. It indicates that the MCE of α-Dy_2S_3 could be controlled

by changing orientation and magnitude of magnetic field.

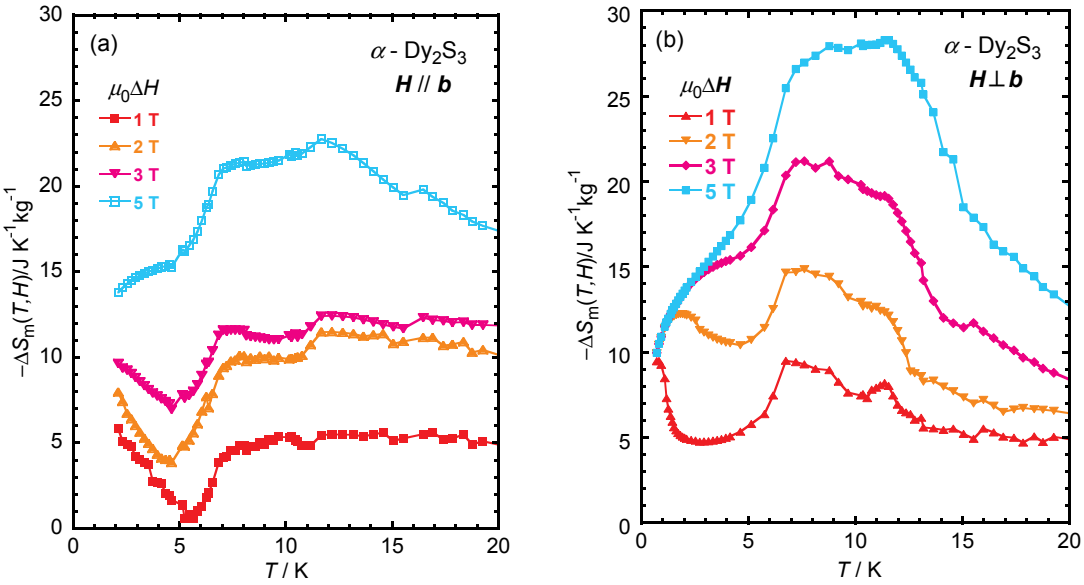

Fig. 10 Temperature dependence of the magnetic entropy change for α-Dy_2S_3 single crystals in magnetic field change within 5 T ***H*//*b*** (a) and ***H*⊥*b*** (b).

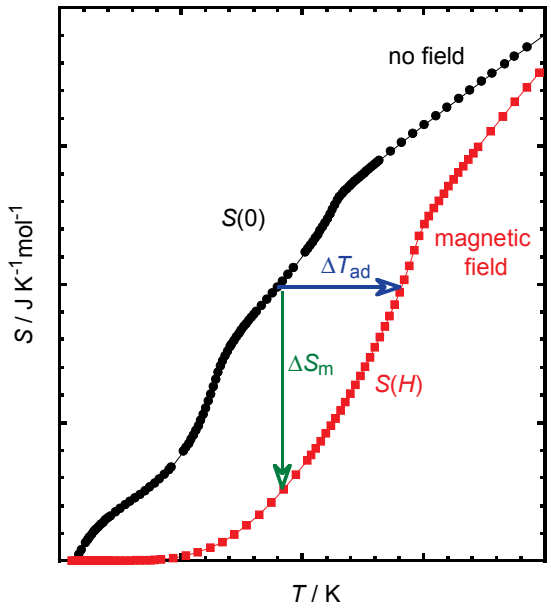

Fig. 11 The description for the MCE in terms of both the isothermal magnetic entropy change ΔS_m and the adiabatic temperature change ΔT_{ad}.

Here, the ΔT_{ad} of α-Tb_2S_3 and α-Dy_2S_3 will be discuss. In general, the ΔT_{ad} can be estimated from the temperature dependence of total entropy [21], which can be written as the following equation,

$$\Delta T_{ad} = T_{S(H)} - T_{S(0)=S(H)} \quad , \tag{7}$$

and is shown in Fig. 11. The temperature dependence of ΔT_{ad} for α-Tb_2S_3 as shown in Fig. 12(a) and (c) can be obtained from the results shown in Fig. 6(a) and (b). However, since α-R_2S_3 (R = Tb, Dy) compounds exhibit two successive AFM transitions, the behavior of $S_m(T)$ is complicated as seen in Fig. 6 and Fig. 7. Therefore, the $\Delta T'_{ad}$ can be calculated by using the equation,

$$\Delta T'_{ad} = -\frac{T}{c_p}\Delta S_m \quad . \tag{8}$$

The calculated results for α-Tb_2S_3 are shown in Fig. 12(b); $\boldsymbol{H}//\boldsymbol{b}$ and (d); $\boldsymbol{H}\perp\boldsymbol{b}$. Comparing Fig. 12(a, c) and (b, d), the features of adiabatic temperature change curves, namely $\Delta T_{ad}(T)$ and $\Delta T'_{ad}(T)$, are similar qualitatively. However, the values of ΔT_{ad} and $\Delta T'_{ad}$ in the case of magnetic field change below 3 T are slightly different. In the case of $\mu_0\Delta H$ = 4 T ($\boldsymbol{H}\perp\boldsymbol{b}$), the values of differences between those are larger. It might be due to that we assumed the constant value for the C_p in the evaluation of $\Delta T'_{ad}(T)$ using Eq. (8). In the following parts, the data of ΔT_{ad} will be used to discuss. It should be pointed out that the value of the ΔT_{ad} curves are ended around T = 10 K because the $S'_m(T)$ have a limitation temperature 20 K in our measurement. In Fig. 12(a), the curves of $\Delta T_{ad}(T)$ in the magnetic field change of 3 T show valleys at the temperature range about 7 to 12 K. When the magnetic field increases to 2 T, the value of ΔT_{ad} firstly decreases. Then, it increases when the field is up to 4 T. In general, the adiabatic temperature change for MCE material is positive and increases when magnetic field change increases. It is named normal adiabatic temperature change. However, inverse adiabatic temperature have been observed in α-Tb_2S_3 compound in a widely temperature range between T_{N1} to T_{N2}. The maximal ΔT_{ad} of α-Tb_2S_3 is 10.6 K at T = 8.7 K in magnetic field of 4 T ($\boldsymbol{H}//\boldsymbol{b}$), although the values are limited because of experiment data below 20 K. For α-Tb_2S_3 in $\boldsymbol{H}\perp\boldsymbol{b}$, there exists a peak of ΔT_{ad} at about 5 K and a valley at about 12 K in $\mu_0\Delta H$ = 2, 2.5 and 3 T. However, when the magnetic field change is 4 T, the value of ΔT_{ad} constantly increases with increasing temperature. The maximal ΔT_{ad} of α-Tb_2S_3 is 10.0 K at T = 10.2 K in magnetic field change of 4 T ($\boldsymbol{H}\perp\boldsymbol{b}$).

Here, we have to point out some issues on our estimation of the adiabatic temperature change ΔT_{ad} and $\Delta T'_{ad}$. The $\Delta T_{ad}(T)$ and $\Delta T'_{ad}(T)$ for 4 T in Fig. 12(c) and (d) shows divergence behavior. We consider that such behavior is somewhat strange. We admit there exist imperfection in the two estimation methods. The first method estimating ΔT_{ad} directly from the figure of $S'_m(T)$ is so simple, however it is suspicious whether we can applicate it for successive magnetic transition systems. As for the second method estimating $\Delta T'_{ad}$ from Eq. (8), we might have to consider the temperature dependence of C_p. However, we believe the behavior of ΔT_{ad} and $\Delta T'_{ad}$

without divergence in the

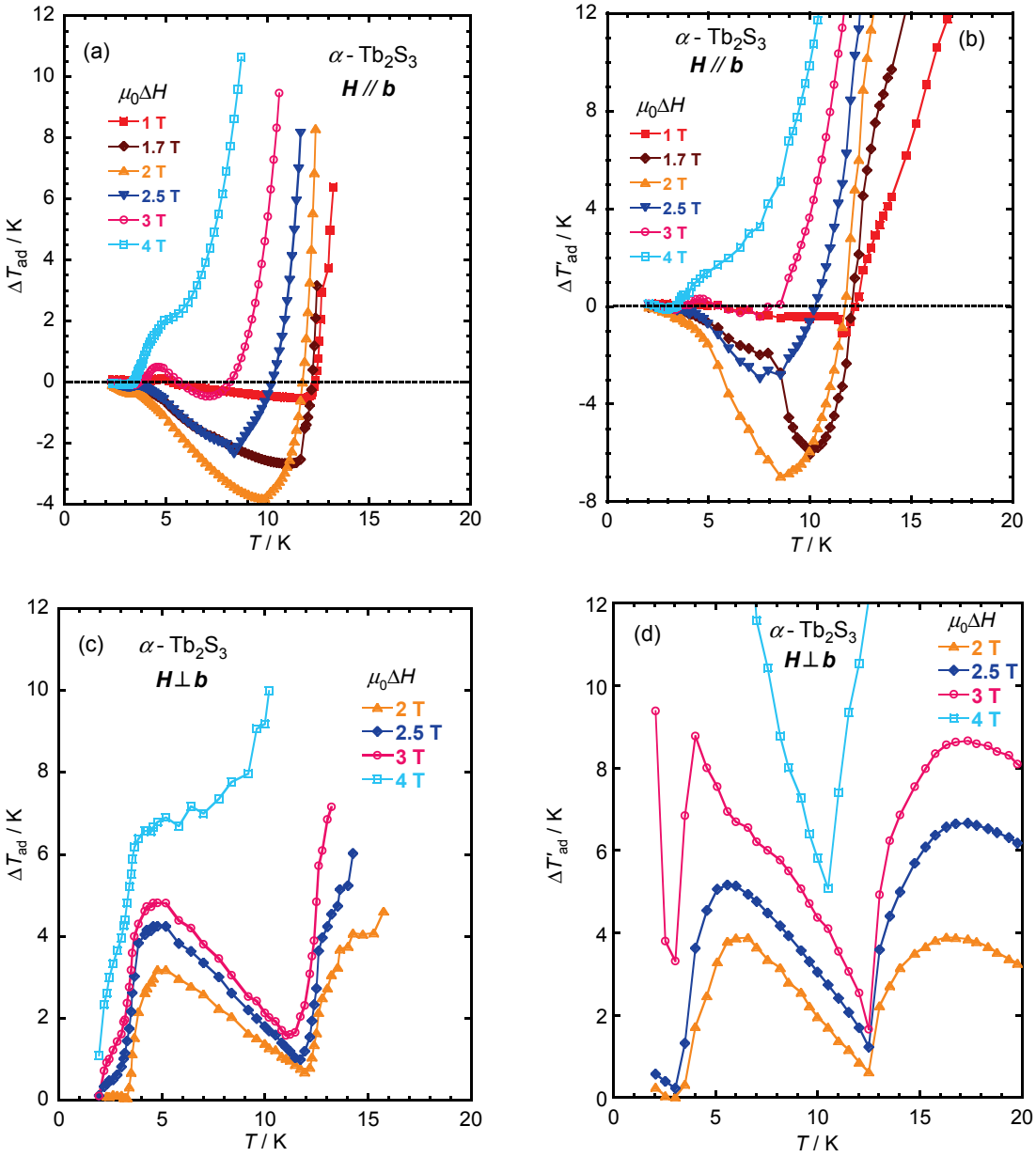

Fig. 12 Temperature dependence of the adiabatic temperature change ΔT_{ad} estimated from magnetic entropy data for α-Tb_2S_3 single crystal in magnetic field change within 4 T; ***H*//*b*** (a) and ***H*⊥*b*** (c). The $\Delta T'_{ad}$ from Eq. (8); ***H*//*b*** (b) and ***H*⊥*b*** (d).

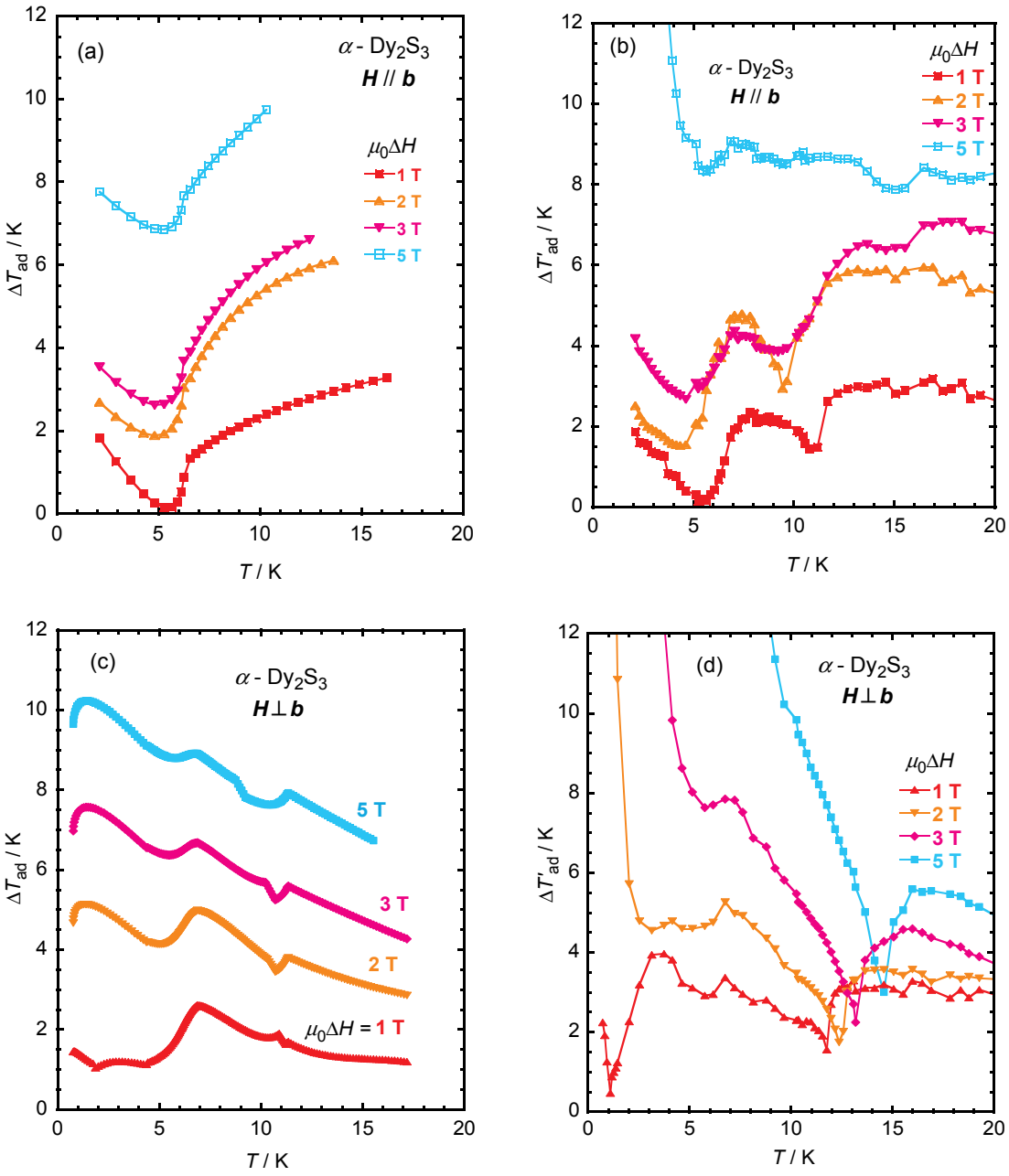

Fig. 13 Temperature dependence of the adiabatic temperature change ΔT_{ad} estimated from magnetic entropy data for α-Dy_2S_3 single crystal in magnetic field change within 5 T; ***H*//*b*** (a) and ***H*⊥*b*** (c). The $\Delta T'_{ad}$ from Eq. (8); ***H*//*b*** (b) and ***H*⊥*b*** (d).

relatively low magnetic field is valid qualitatively.

Fig. 13 is the temperature dependence of ΔT_{ad} and $\Delta T'_{ad}$ of α-Dy_2S_3 in magnetic field change within 5 T in ***H*//*b***; (a, b) and ***H*⊥*b***; (c, d). Also in this case of α-Dy_2S_3, it can be seen that the features of $\Delta T'_{ad}$ curves resemble that of ΔT_{ad} curves qualitatively. Fig. 13 (b) and (d) exhibit divergence behaviors as well as α-Tb_2S_3, especially in the

higher magnetic fields. Thus, the MCE will be discussed by using the value from Fig. 13 (a) and (c). The larger the magnetic field change is, The higher the value of ΔT_{ad} is in both cases of $\boldsymbol{H}//\boldsymbol{b}$ and $\boldsymbol{H}\perp\boldsymbol{b}$. In Fig. 13(a), it is obvious that the $\Delta T_{ad}(T)$ curves show valleys around T =5.5 K. The maximal value of ΔT_{ad} is 9.7 K at T = 10.3 K in magnetic field of 5 T ($\boldsymbol{H}//\boldsymbol{b}$). In the case of $\boldsymbol{H}\perp\boldsymbol{b}$ in Fig. 13(c), the value of ΔT_{ad} in any curves tends to decrease with increasing the temperature. We can also see that there exists two minimal values around 7 and 11 K, which are close to T_{N2} and T_{N1}. The maximal value of ΔT_{ad} is 10.2 K at T = 1.2 K in magnetic field of 5 T ($\boldsymbol{H}\perp\boldsymbol{b}$).

Table 1 The comparison of maximal magnetic entropy change and adiabatic temperature change of MCE materials in the temperature range below 20 K.

Compounds	Magnetic field / T	Maximal ΔS_m at T_1			Maximal ΔT_{ad} at T_2	
		ΔS_m /J kg^{-1} K^{-1}	ΔS_m /J m^{-3} K^{-1}	T_1 / K	ΔT_{ad} / K	T_2 / K
α-Tb_2S_3	4 ($\boldsymbol{H}//\boldsymbol{b}$)	11.7	73.3	20.0	10.6	8.7
	4 ($\boldsymbol{H}\perp\boldsymbol{b}$)	12.0	75.2	13.6	10.0	10.2
α-Dy_2S_3	5 ($\boldsymbol{H}//\boldsymbol{b}$)	22.8	149.0	11.7	9.7	10.3
	5 ($\boldsymbol{H}\perp\boldsymbol{b}$)	28.3	185.0	11.4	10.2	1.2
ErN [22]	5	34.7	370.0	7.0	8.4	16.0
HoN [23]	5	28.3	291.0	18.0	10.2	23.0
$ErAl_2$ [23]	5	38.7	240.0	11.1	-	-
HoCoAl [23]	5	22.6	171.0	10.0	-	-
$GdPd_2Si$ [23]	5	15.17	142.0	17.0	8.6	17.0

The maximal magnetic entropy changes and adiabatic temperature changes of two single crystals below 20 K were listed in Table 1 and compared with the conventional MCE materials [21, 22]. The values of ΔS_m expressed by two cases unit mass (kg) and unit volume (m^3) considering varies uses of the MCE materials. From Table 1, it can be seen that the magnetic entropy change ΔS_m and adiabatic temperature change ΔT_{ad} of α-Tb_2S_3 and α-Dy_2S_3 are not so much higher compared with conventional related materials, although the values of $\Delta S_m(T)$ and $\Delta T_{ad}(T)$ in the case of unit mass are comparable. However, as mentioned in Fig. 10-13, the value and shape of ΔS_m and ΔT_{ad} are extremely different between in the magnetic field of $\boldsymbol{H}//\boldsymbol{b}$ and $\boldsymbol{H}\perp\boldsymbol{b}$ for α-Tb_2S_3 and α- Dy_2S_3 single crystals. Using this feature as an advantage, it may be possible that the refrigerating capacity, thermal absorption capacity will be controlled by changing

magnitude and orientation of magnetic field on the α-Tb_2S_3 and α-Dy_2S_3 single crystals.

4 Conclusion

In this work, the specific heat of α-Tb_2S_3 and α-Dy_2S_3 single crystals in different magnetic field ($\boldsymbol{H} \perp \boldsymbol{b}$ and $\boldsymbol{H} // \boldsymbol{b}$) were investigated. From the temperature dependence of specific heat of α-Tb_2S_3 in no magnetic field, we have found that the ground state of each Tb site is quasi-doublet. For α-Dy_2S_3, the temperature dependence of specific heat shows that there still exists finite value of C_m at 0.7 K in no magnetic field, which means the magnetic entropy remains. The magnetic entropy can be released in $\mu_0 H$ = 1 T due to some kind of order at 1.0 K. From the consideration of temperature dependence of magnetic entropy, it can be obtained that the ground state of one Dy site in which Dy^{3+} moments order at T_{N2} is a quasi-quartet ground state. In addition, we estimated the MCE expressed by magnetic entropy change and adiabatic temperature change of α-Tb_2S_3 and α-Dy_2S_3 compounds. Only in the case of $\boldsymbol{H} // \boldsymbol{b}$, the α-$Tb_2S_3$ exhibits inverse MCE below 12 K within magnetic field change of 3 T. It have been found that the value and shape of ΔS_m and ΔT_{ad} are extremely different between in the magnetic field of $\boldsymbol{H} // \boldsymbol{b}$ and $\boldsymbol{H} \perp \boldsymbol{b}$ for α-Tb_2S_3 and α-Dy_2S_3 single crystals. Therefore, the MCE of α-Tb_2S_3 and α-Dy_2S_3 can be controlled by magnitude and orientation of magnetic field. As a consequence, it may be possible that the refrigerating capacity, thermal absorption capacity will be controlled by changing magnitude and orientation of magnetic field on the α-Tb_2S_3 and α-Dy_2S_3 single crystals.

References:

[1] V. K. Pecharsky, K. A. Gschneidner, Giant Magnetocaloric Effect in $Gd_5(Si_2Ge_2)$, Phys. Rev. Lett. **78** (1997) 4494.

[2] O. Tegus, E. Brück, K. H. J. Buschow, F. R. de Boer, Transition-metal-based magnetic refrigerants for room-temperature applications, Nature **415** (10) (2002) 150–152.

[3] X. Chen, Y. G. Chen, Y. B. Tang, Influence of iron on phase and magnetic property of the $LaFe_{11.6}Si_{1.4}$ compound, J. Rare Earth. **29** (4) (2011) 354–358.

[4] N. K. Singh, K. G. Suresh, A. K. Nigam, S. K. Malik, A. A. Coelho, S. Gama, Itinerant electron metamagnetism and magnetocaloric effect in RCo_2-based laves phase compounds, J. Magn. Magn. Mater. **317** (2007) 68–79.

[5] M. Patra, S. Majumdar, S. Giri, Y. Xiao, T. Chatterji, Magnetocaloric effect in RAl_2 (R = Nd, Sm, and Tm): Promising for cryogenic refrigeration close to liquid helium temperature, J. Alloy. Compd. **531** (2012) 55–58.

[6] S. Ebisu, Y. Iijima, T. Iwasa, S. Nagata, Antiferromagnetic transition and electrical

conductivity in α-Gd_2S_3, J. Phys. Chem. Solids **65** (2004) 1113–1120.
[7] A. Kikkawa, K. Katsumata, S. Ebisu, S. Nagata, Phase transition of a frustrated magnet α-Gd_2S_3, J. Phys. Soc. Japan **73** (11) (2004) 2955–2958.
[8] S. Ebisu, M. Narumi, S. Nagata, Anomalous enlargement of electrical resistivity between successive magnetic transitions in α-Gd_2S_3, J. Phys. Soc. Japan **75** (8) (2006) 085002.
[9] S. Ebisu, M. Gorai, K. Maekawa, S. Nagata, Highly anisotropic properties of an antiferromagnetic α-Tb_2S_3 single crystal, AIP Conf. Proc. **850** (2006) 1237–1238.
[10] S. Ebisu, M. Narumi, M. Gorai, S. Nagata, Successive magnetic phase transitions in α-Dy_2S_3 single crystal, J. Magn. Magn. Mater. **310** (2007) 1741–1743.
[11] S. Ebisu, K. Koyama, H. Omote and S. Nagata, High field magnetization processes in single crystal of α-Tb_2S_3 and α-Dy_2S_3, J. Phys.: conf. Ser. **150** (2009) 042027.
[12] S. Ebisu, H. Omote and S. Nagata, Drastic change of the electrical resistivity related to the novel magnetic phase transition in α-Sm_2S_3, J. Phys.: conf. Ser. **200** (2010) 092005.
[13] S. Ebisu, K. Koyama, T. Horikoshi, M. Kokita and S. Nagata, Extremely broad hysteresis in the magnetization process of α-Dy_2S_3 single crystal induced by high field cooling, J. Phys.: conf. Ser., **400** (2012) 032010.
[14] S. Ebisu, Y. Ushiki, S. Takahashi, Specific-heat study on successive magnetic transitions in α-Dy_2S_3 single crystals under magnetic fields, J. Kor. Phys. Soc. **63** (3) (2013) 571–574.
[15] S. Ebisu, T. Nagata, K. Fuji, Y. Shibayama, Magnetism in α-R_2S_3 (R = Pr and Nd) single crystals, J. Phys.: conf. Ser. **568** (2014) 042003.
[16] S. Ebisu, J. Awaka, K. Fuji, Aiming for high performance magnetocaloric materials, in: Memoirs of the Muroran Institute of Technology, **63** (2014) 33–36.
[17] S. Ebisu, K. Fuji, Q. Guo, M. Miyazaki, Metastable magnetic phase induced by rotation of α-Dy_2S_3 single crystal in magnetic field, J. Magn. Magn. Mater. **444** (2017) 140–145.
[18] M. Matsuda, A. Kikkawa, S. Ebisu, S. Nagata, Neutron diffraction study of α-Gd_2S_3, J. Phys. Soc. Japan **74** (5) (2005) 1412–1415.
[19] M. Matsuda, K. Kakurai, S. Ebisu, and S. Nagata, Successive magnetic phase transitions in α-Tb_2S_3 studied by Neutron Diffraction technique, J. Phys. Soc. Jpn. **75** (2006) 074710.
[20] X. Q. Zheng, Z. Y. Xu, B. Zhang, F. X. Hu, B. G. Shen, The normal and inverse magnetocaloric effect in $R$$Cu_2$ (R = Tb, Dy, Ho, Er) compounds, Journal of Magnetism and Magnetic Materials **421** (2017) 488–452.

[21] V. K. Pecharsky, K. A. Gschneidner, Jr., A. O. Pecharsky and A. M. Tishin, Thermodynamics of the magnetocaloric effect, Physical Review B **64** (2001) 144406.
[22] Y. Hirayama, N. Tomioka, S. Nishio, N. Kusunose, T. Nakgawa, K. Kamiya, T. Numazawa, T. A. Yamamoto, Magnetocaloric effects, specific heat and adiabatic temperature change of $Ho_xEr_{1-x}N$ (x = 0.25, 0.5, 0.75) J. Alloy. Compd. **462** (2008) L12-L15.
[23] K. A. Gschneidner, V. K. Pecharsky and A. O. Tsokol, Recent developments in magnetocaloric materials, Rep. Prog. Phys. **68** (2005) 1479-1539.